Faraday Discuss., 1998, **110**, 287–300

Eley–Rideal and hot-atom dynamics of HD formation by H(D) incident from the gas phase on D(H)-covered Cu(111)

Dmitrii V. Shalashilin,[a]† Bret Jackson[a] and Mats Persson[b]*

[a] *Department of Chemistry, University of Massachusetts, Amherst, MA 01003, USA*
[b] *Department of Applied Physics, Chalmers/Göteborg University, S-412 96, Göteborg, Sweden*

We have performed a quasi-classical molecular dynamics study of the reaction dynamics of HD formation by H or D atoms incident from the gas phase on a D or H-covered Cu(111) surface. A key ingredient has been the construction of a model potential-energy surface (PES) that has been exclusively based on results from total energy calculations using the density functional scheme. Our preliminary study supports the Rettner–Auerbach scenario that a significant fraction of the reactions occurs *via* hot-atom pathways as opposed to Eley–Rideal pathways, in which the incident atom reacts directly with the adsorbed atom. The calculated reaction probabilities and ro-vibrational distributions are in good agreement with the measured distributions. As observed experimentally on other metal surfaces, we also find that the incident atom induces secondary reactions among the adsorbates, producing either H_2 or D_2 molecules. The magnitude and the isotope dependence of the calculated secondary reaction probabilities are in good agreement with measured values.

1 Introduction

Numerous recent experiments have demonstrated the existence of Eley–Rideal (ER) reactions on both metal and semiconductor surfaces.[1–20] Unlike a Langmuir–Hinshelwood reaction, where both reactants are initially adsorbed onto and are in thermal equilibrium with the surface, an ER reaction takes place between an adsorbed species and one entering directly from the gas phase. In many of these experiments, beams of H(g) or D(g) react with H, D or halogens adsorbed onto single-crystal surfaces. The adsorbate–metal bonds for these systems are *ca.* 2–3 eV, while the molecular bonds formed in the products are roughly twice that. Thus, while the Langmuir–Hinshelwood reaction would be nearly thermoneutral, the ER pathway has an exothermicity of *ca.* 2–3 eV for these reactions, the signature of an ER process. The scattered product distribution can also exhibit some sensitivity to the details of the incident beam.

Several quantum and quasi-classical studies have been made of ER reactions,[21–30] and much has been learned. The most thoroughly studied system is H(g) + H/Cu(111) and its isotopic variants.[24,29] There have also been a large number of experimental and theoretical studies of the dynamics of dissociative adsorption of H_2 on Cu(111),[31] all of which can be of value in the construction of the PES. Both quantum and quasi-classical calculations[25,27,29] have been in reasonable agreement with the detailed product state distributions measured by Rettner and Auerbach.[5,8] However, there is a large discrepancy between the measured and theoretical cross-sections. While the calculations give

† On leave from the Institute of Chemical Physics, Russian Academy of Science, 117334 Moscow, Russian Federation.

cross-sections of the order of 0.5 Å^2, the experiments suggest a cross-section of roughly an order of magnitude larger, with about half of the incident atoms undergoing an ER reaction for an initial coverage of half a monolayer. It has been suggested[8,28,29] that a significant fraction of these reactions occur *via* hot-atom pathways,[32] as opposed to direct ER. That is, the incident H atom does not react directly with an adsorbed H as it enters from the gas phase, but is trapped onto the surface first. Extensive quasi-classical studies of H-atom trapping on bare and H-covered Cu(111) surfaces[29,33,34] have shown that the probability of being trapped is closed to unity, with the incident atom scattering from the corrugation and/or an adsorbate into a bound state (normal to the surface). Because of the small H-to-metal atom mass ratio, the dissipation of energy into the solid is slow,[33,34] and by the time these trapped hot-atoms react they are still well above the H-metal ground state. For instance, classical dynamics studies[33] suggest that an incident H atom travels more than 6 lattice spacings before it becomes equilibrated with the lattice. As a result, the products are expected to be nearly as 'hot' as those resulting from direct ER reactions.

In this paper, we examine this scenario of direct Eley–Rideal and hot-atom reactions in detail using quasi-classical molecular dynamics calculations. Our construction of the PES is more ambitious than in previous studies, since it is based only on first principle total energy studies and, unlike these earlier works, we simulate a surface coverage of one adsorbate per two unit cells, equal to that in the experiments. In the next section, we describe our density functional calculations of the total energy of the H + H/Cu(111) interaction. We then use the results of these calculations to construct a reactive PES based on a corrugated Morse function. In this section, we also describe the quasi-classical calculations that we then use in Section 3 to examine the various pathways to reaction and trapping of H(D)(g) incident on a D(H)-covered Cu(111) surface. Comparison is made with the experiments of Rettner and Auerbach, as well as other studies of H(g) + H(ads) on metals. We conclude with a brief summary.

2 Theory

2.1 Many-body PES for hydrogen on Cu(111)

We construct our model PES for a system of hydrogen atoms on a rigid substrate by considering the interaction between two hydrogen atoms on Cu. At the coverage of interest in this work, we find that three or more H atoms are never sufficiently close together at any one time to make three-body and higher interactions important. It is thus sufficient to expand our interaction potential up to two-body terms as,

$$V(\{\boldsymbol{r}_i\}) = \sum_i V_{\mathrm{a}}(\boldsymbol{r}_i) + \sum_{i<j} V_{\mathrm{aa}}(\boldsymbol{r}_i, \boldsymbol{r}_j) \tag{2.1}$$

where $\boldsymbol{r}_i$ is the position of atom i, the one-body term $V_{\mathrm{a}}(\boldsymbol{r}_i)$ is the interaction of a single H atom with the surface and the two-body term $V_{\mathrm{aa}}(\boldsymbol{r}_i, \boldsymbol{r}_j)$ describes the interaction between two hydrogen atoms in the presence of the surface. These two potential terms can be determined by considering the case of only two H atoms, for which eqn. (2.1) reduces to

$$V(\boldsymbol{r}_1, \boldsymbol{r}_2) = V_{\mathrm{a}}(\boldsymbol{r}_1) + V_{\mathrm{a}}(\boldsymbol{r}_2) + V_{\mathrm{aa}}(\boldsymbol{r}_1, \boldsymbol{r}_2) \tag{2.2}$$

To determine an accurate form for $V(\boldsymbol{r}_1, \boldsymbol{r}_2)$, we have performed total energy calculations, based on density functional theory (DFT), for several configurations of two hydrogens over Cu(111) that are relevant for the ER reaction of a gas-phase H atom with an adsorbed H atom. We have been motivated by the success of several groups[35,36] who have used such calculations to examine the regions of $V(\boldsymbol{r}_1, \boldsymbol{r}_2)$ that are relevant for the dissociation of H_2 on metal surfaces. Such calculations cannot provide a complete

PES that can be used in dynamics calculation and it is necessary to develop a model PES.

A model potential that is both simple and chemically sound is the LEPS (London, Eyring, Polanyi and Sato) PES. An LEPS-PES that was first adapted to reactions at surfaces by McCreery and Wolken[37] and has been widely used is provided by,

$$V(\boldsymbol{r}_1, \boldsymbol{r}_2) = U_a(\boldsymbol{r}_1) + U(\boldsymbol{r}_2) + U_m(r) - \sqrt{Q_m(r)^2 + [Q_a(\boldsymbol{r}_1) + Q_a(\boldsymbol{r}_2)]^2 - Q_m(r)[Q_a(\boldsymbol{r}_1) + Q_a(\boldsymbol{r}_2)]} \quad (2.3)$$

where $r = |\boldsymbol{r}_1\text{-}\boldsymbol{r}_2|$. The terms U_σ and Q_σ, σ = a or m, are defined as

$$U_\sigma = \frac{1}{4(1+\Delta_\sigma)} D_\sigma\{(3+\Delta_\sigma)\exp[-2\alpha_\sigma(r_\sigma - r_{\sigma 0})] - (2+6\Delta_\sigma)\exp[-\alpha_\sigma(r_\sigma - r_{\sigma 0})]\} \quad (2.4)$$

$$Q_\sigma = \frac{1}{4(1+\Delta_\sigma)} D_\sigma\{(1+3\Delta_\sigma)\exp[-2\alpha_\sigma(r_\sigma - r_{\sigma 0})] - (6+2\Delta_\sigma)\exp[-\alpha_\sigma(r_\sigma - r_{\sigma 0})]\} \quad (2.5)$$

where $r_m \equiv r$ is the H—H internuclear distance and $r_a \equiv z_1$ or z_2 are the distances of atoms 1 and 2, respectively, above the surface plane. Because of surface corrugation, the Morse parameters describing the atom–metal interaction, D_a, α_a and r_{a0}, depend upon the lateral position of the atom in the surface unit cell. When r is large and the hydrogens do not interact, $V(\boldsymbol{r}_1, \boldsymbol{r}_2)$ reduces to $V_a(\boldsymbol{r}_1) + V_a(\boldsymbol{r}_2)$, where the single atom–metal interaction $V_a = U_a + Q_a$ is a corrugated Morse potential:

$$V_a(\boldsymbol{r}) = D_a(\boldsymbol{R})(\exp\{-2\alpha_a(\boldsymbol{R})[z - z_0(\boldsymbol{R})]\} - 2\exp\{-\alpha_a(\boldsymbol{R})[z - z_0(\boldsymbol{R})]\}) \quad (2.6)$$

and $\boldsymbol{R}$ is the lateral coordinate of the H atom. The LEPS-PES also reduces to a Morse potential, $V_m(r) = U_m + Q_m$, for large distances of the two H atoms from the surface. The potential-energy curve for the isolated hydrogen molecule is thus

$$V_m(r) = D_m\{\exp[-2\alpha_m(r - r_0)] - 2\exp[-\alpha_m(r - r_0)]\} \quad (2.7)$$

The remaining so-called Sato parameters, Δ_a and Δ_m in eqn. (2.3), determine the reactive part of the PES. We now proceed to show how all these parameters have been determined from calculated total energies within DFT for an isolated molecule and various configurations of a single H atom and two interacting H atoms on a Cu(111) surface.

The total energy calculations are based on DFT using the generalized gradient approximation (GGA) for the exchange and correlation energy. The total energy was computed in a super-cell geometry using a plane-wave and pseudo-potential code.[38] The choice of the plane wave set and the super cell were based on the experience gained by Hammer and co-workers[35] in their calculations of PES for hydrogen dissociation on Cu(111). This choice was also used in the calculations by Strömqvist and co-workers[33] of potential-energy curves for the interaction of a single H atom with this surface. Here, it is sufficient to mention that the Cu(111) was represented by a slab of four atomic layers and that each substrate layer contained three Cu atoms. All 3d states of Cu were included and the hydrogen atom was represented by its bare Coulomb potential. More details and results of these calculations will be reported elsewhere.[39]

The construction of the corrugated Morse potential $V_a(\boldsymbol{r})$ in eqn. (2.6) is based on DFT-GGA results for the potential energy of a single H atom over four high-symmetry surface sites on Cu(111). The results for hollow, bridge and top sites by Strömqvist and co-workers[33] showed that the H—Cu(111) interaction is rather corrugated, both geometrically and energetically. For example, the potential-energy minimum above the top site is located 0.6 Å farther out than the chemisorption minimum at the hollow site and is 0.5 eV less deep than the potential-energy minimum at the hollow site, whereas the diffusion barrier at the bridge site is only 0.15 eV and is located only 0.1 Å outside the equilibrium position. The extracted chemisorption bond parameters from the calculated

potential-energy curves were found to be in good agreement with available experimental data. A somewhat unexpected finding of these calculations was that absorption into a subsurface site is non-activated close to a hollow site: the area of this region is found from an interpolation of the calculated curves to be a small fraction of the surface unit cell, only *ca.* 14% at zero incidence energy. The corrugated Morse potential is strictly repulsive close to the surface, so subsurface absorption is ignored in this work. Away from this absorption region, however, the corrugated Morse potential agrees well with the calculated potential. A Morse potential in z was fit by least squares to the calculated potential-energy points for H over each of four sites: the top, hollow and bridge sites, as well as a site located halfway between the hollow and atop sites. The fitted Morse parameters for these four surface sites, which evenly cover the unit cell, are listed in Table 1. We interpolated between these high symmetry sites by expanding D_a, α_a and r_{a0} in a Fourier series over reciprocal lattice vectors, $\boldsymbol{G}_{hk}$, illustrated here for $D_a(\boldsymbol{R})$ as

$$D_a(\boldsymbol{R}) = \sum_{hk} D_{hk} \exp(-i\boldsymbol{G}_{hk} \cdot \boldsymbol{R}) \tag{2.8}$$

Using the symmetry of the (111) surface layer, we were able to group sets of terms with equivalent coefficients. For each expansion, we retained the four largest unique coefficients,[40] corresponding to 19 terms in eqn. (2.8). These four coefficients for each Morse parameter were then chosen to reproduce the corresponding Morse fit parameters listed for the four sites in Table 1.

The Morse potential describing the isolated molecule is based on our calculated DFT-GGA energies. To obtain a good description of the dissociation limit, as has been discussed in the literature,[41] it was found to be necessary to include spin polarization in the calculation for $r \gtrsim 1.8$ Å. In comparison with experiments, our calculated DFT-GGA value for the potential-energy minimum is *ca.* 0.26 eV smaller in magnitude than the experimental value. We find that this discrepancy is not simply an effect of our chosen plane-wave basis set but rather a limitation of DFT-GGA.[42] The Morse parameters obtained by a least-square fit to the calculated values are tabulated in Table 1.

We determine the Sato parameters, and assess the overall accuracy of our model PES, by considering DFT-GGA calculations of four two-dimensional sections of

Table 1 Morse potential parameters extracted from DFT-GGA calculations

σ	D_σ/eV	$r_{\sigma 0}$/Å	α_σ	rms/eV
m	4.53	0.76	2.14	0.12
a: hollow	2.37	0.95	1.01	0.032
a: bridge	2.22	1.08	1.00	0.032
a: top	1.84	1.52	1.72	0.006
a: hollow/top	1.93	1.33	1.44	0.089

All these parameters were obtained by a least-square fit to potential-energy curves calculated using DFT-GGA. For the molecule, the range of calculated interatomic distances was from 0.4 to 3 Å. For the hollow, bridge, top and the hollow/top sites the ranges of the calculated atom–surface distances were 0.4 to 1.4 Å, 0.4 to 1.45 Å, 1.1 to 1.9 Å, and 0.8 to 2.0 Å, respectively. The errors in the root-mean-square sense are also indicated. The values for the parameters obtained for the so-called hcp and fcc configurations of the hollow site are essentially the same within the rms error.

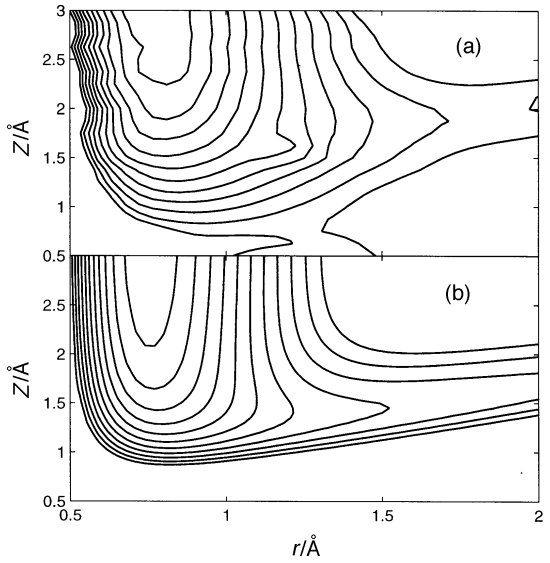

Fig. 1 Contour plots of collinear sections of the PES for two hydrogen atoms on a Cu(111) surface. (a) Based on an irregular set of energy points calculated within DFT-GGA. (b) Corrugated LEPS-PES based on potential parameters obtained from calculated energy points within DFT-GGA for an isolated hydrogen molecule, a single hydrogen atom interacting with a Cu(111) surface and from various configurations of two hydrogen atoms on a Cu(111) surface. $r = z_2 - z_1$ and $Z = (z_1 + z_2)/2$ where z_1 and z_2 are the perpendicular distances of the adsorbed and the incident atoms above the hollow site. The contours range from 0 to 2.2 eV with a spacing of 0.2 eV.

$V(\boldsymbol{r}_1, \boldsymbol{r}_2)$ that are relevant for an ER reaction. In Fig. 1, we show a contour plot of the collinear section of the calculated PES, in which both hydrogen atoms are located at various distances above the hollow site. This section has a simple elbow shape with no energy barriers along the minimum-energy path from the entrance channel, corresponding to an incident H atom and a chemisorbed H atom, to the exit channel, corresponding to a hydrogen molecule. The potential-energy release in this reaction is *ca.* 2.1 eV, of which a substantial fraction (*ca.* 1 eV) is in the entrance channel. To describe properly the interaction of the incident H atom with the adsorbed H atom, it was necessary to perform spin-polarized calculations for distances larger than *ca.* 1.4 Å between the two atoms. For instance, when using unpolarized GGA, the potential-energy release is *ca.* 1 eV larger than using spin-polarized GGA.

We have determined the Sato parameters by a least-square fit of the corrugated LEPS-PES to the calculated energy points for four two-dimensional sections of $V(\boldsymbol{r}_1, \boldsymbol{r}_2)$. The resulting values for Δ_a and Δ_m from such a fit to the collinear configuration of the PES with potential energies less than 2 eV are shown in Table 2. To see whether these Sato parameters are sensitive to the chosen set of configurations of the H atom, we have calculated total energy points for three more two-dimensional and discrete sets of configurations. One set, denoted by BH, differs from the collinear set, denoted by C, only by the incident atom being located above the bridge site instead of above the hollow site. In the other two sets, one H atom is located at the chemisorption minimum and the other H atom is located in one of the two planes spanned by the surface normal and the direction from hollow to top site (denoted by HT) or from hollow to the nearest-neighbouring hollow site (denoted by HBH), respectively. As can be seen from Table 2, the least-square fit to each set of calculated energy points gives similar values for the Sato parameters and rms errors. This result gives us some confidence that our model

Table 2 Sato parameters of the corrugated LEPS-PES

sets	Δ_a	Δ_m	rms/eV
C	0.13	−0.26	0.19(0.19)
HB	0.15	−0.26	0.16(0.19)
HBH	0.10	−0.20	0.23(0.23)
HT	0.06	−0.15	0.13(0.15)
global	0.10	−0.20	0.17

These parameters were determined by a least-squares fit of the corrugated LEPS-PES to various two-dimensional and discrete sets of energy points as calculated by DFT-GGA. The root mean square errors are also indicated. The results from a global fit to all sets are also included. The values within parentheses refer to the rms error for each set using the Sato parameters obtained from the global fit. The configurations of the hydrogen atoms for all the sets are defined in the text.

PES is chemically sound. The final values for the Sato parameters that we use in our dynamics calculations are obtained from a global fit to all four sets of energy points and are also tabulated in Table 2.

To illustrate the quality of the resulting LEPS-PES, we have made a direct comparison, in Fig. 1, of the contour plots of the collinear sections (set C) of this PES with the calculated PES. The overall agreement is good, in view of the limited number of parameters in the LEPS-PES. There are two notable differences between the two PESs. First, in the LEPS-PES, the interaction in the entrance channel is more long-ranged than in the DFT-GGA PES. Secondly, the DFT-GGA has a saddle point associated with absorption of the H atom into a subsurface site, which is absent in the LEPS-PES. Another indication of the quality of the LEPS-PES is provided by considering a two-dimensional section that is relevant for dissociation of the molecule: the potential energy as a function of the centre-of-mass distance from the surface and the inter-atomic distance when the molecule is oriented parallel to the surface above the bridge site, with the hydrogen atoms pointing towards their chemisorption sites. The constructed LEPS-PES gives a value of 0.72 eV and a position $(r, z) = (1.06, 1.20)$ Å for the activation barrier for dissociation. These values are both close to the values of 0.54 eV and (1.1, 1.2) Å, respectively, calculated by Hammer and co-workers[35] using DFT-GGA.

Finally, we would like to comment on earlier models of the PES for the interactions of two hydrogen atoms on Cu(111). An early attempt by us[24] was based on a flat-surface approximation, no surface corrugation of the H—Cu interaction; the choice of potential parameters was guided by measured values for the H—Cu vibrational frequency and binding energy, and the Sato parameters were chosen to reproduce the accepted view about the activation barrier for dissociation being late in the entrance channel with a barrier of *ca.* 0.6 eV. The resulting Sato parameters, $\Delta_a = 0.2$ and $\Delta_m = -0.2$, are close to the values that we obtain here. This PES was later refined by corrugating the LEPS potential with a corrugation function for the H—Cu Morse potential that was based on the DFT-GGA calculations for H on Cu(111), and the same values were kept for the Sato parameters.[29] A corrugated LEPS-PES was also constructed by Dai and Zhang[43]

in their quantum dynamics study of dissociative adsorption. Their construction was partly based on the DFT-GGA calculations by Hammer and co-workers[35] but they were not certain that their choice of parameters was accurate or even consistent without sufficient first-principles data. However, it turns out that their H—Cu potential is very similar to our deduced Morse potentials over hollow, bridge, and top sites and that their deduced values for the Sato parameters, $\Delta_a = 0.1$ and $\Delta_m = -0.15$, are very close to our deduced values in Table 1. One important difference between their PES and the one developed in this work is that they based the Morse potential for the isolated hydrogen molecule on experiments.

2.2 Quasi-classical dynamics

In this work, we simulate an H or D atom incident on a D or H-covered Cu(111) surface, where the coverage is one adsorbate per two unit cells, equal to that of the experiments. This coverage corresponds to one adsorbed atom for every four hollow sites. Our earlier studies have shown that the hot-atoms formed by scattering from the corrugation and/or adsorbates can travel over large distances at high speeds. Thus, although our incident atom is aimed at random points within an array of four surface unit cells, we must allow it to roam over a large area. One way of doing this calculation is to cover a finite surface area with adsorbed hydrogens, and impose periodic boundary conditions. Taking a somewhat similar approach, we use a six-by-six rhombic array of 36 surface unit cells, containing 18 adsorbed atoms, and surrounded by perfectly reflecting walls perpendicular to the surface. Thus, when a hot atom approaches the edge of our array, it is reflected back. When an H_2 molecule hits the reflecting wall, only its centre-of-mass translational motion is reflected; ro-vibrational motion is unchanged. Actual trajectories can be determined by 'mirroring' beyond the walls.

We used Hamilton's equations and the velocity Verlet algorithm to evolve the incident atom and all adsorbed atoms. Initially, the incident atom is 7 Å above the surface, at normal incidence, with a translational energy of 70 meV. The adsorbed atoms are initially in the vibrational ground state, with total zero point energies of 0.159 and 0.112 eV, for H and D, respectively. The initial adsorbate oscillator phases are chosen randomly, using a harmonic oscillator approximation for their initial state. The PES is given by eqn. (2.1) and (2.6). The two-body terms, $V_{aa}(\boldsymbol{r}_i, \boldsymbol{r}_j)$, are set equal to zero, except for pairs of hydrogens that satisfy $|\boldsymbol{r}_i - \boldsymbol{r}_j| \leqslant 5$ Å, for which case $V_{aa}(\boldsymbol{r}_i, \boldsymbol{r}_j)$ is defined by eqn. (2.2) and (2.3). Note that this LEPS-based two-H term is actually a three-body reactive potential, where the third body is the metal. Our PES can lead to unphysical results if three or more H atoms are in close proximity. The lack of three-H interaction terms, for example, makes the $H + H_2$ interaction attractive, and can lead to unphysical H_3 formation. This effect can be avoided by restricting each H to a single two-H interaction, or by introducing explicit three-H terms in the potential. However, we have observed that three-H and higher interactions are negligible in these simulations. The nearest-neighbour adsorbates are on opposite sides of a Cu atom, deep in the threefold hollows and, therefore, screened from each other. The next-nearest-neighbour spacing is large at this coverage, and even when adsorbates are knocked loose by the incident atom, they are not seen to be close to more than one other atom at a time.

We have performed a preliminary quasi-classical analysis of the ro-vibrational state of each HD product based on the rigid rotor approximation. In this approximation, the rotational energy E_{rot} is related to the angular momentum J as $J^2/2\mu r_0^2$ where μ is the reduced mass. The vibrational energy E_{vib} was then determined from the energy of internal motion, E_{int}, as $E_{vib} = E_{int} - E_{rot}$. The vibrational and rotational quantum numbers, v and j, for this state were determined by the correspondence $v + \frac{1}{2} = \eta/\hbar$ and $j = J/\hbar$, where the action η of the vibrational motion was evaluated from E_{vib} using the exact quadratic relation for the Morse oscillator. Integer values for v and j were obtained by a

standard binning procedure. We find that 4000 total runs, each involving 19 atoms, are sufficient to generate good statistics.

Phonon effects are not included in this first finite-coverage study, although efficient quasi-Langevin techniques have been developed to do this.[34] Our studies of hot-atom behaviour have shown that energy loss to the phonons is very slow due to the small H-to-Cu mass ratio, and at these coverages the dominant hot-atom energy loss mechanism is due to collisions with the adsorbates, where the mass ratio is much more favourable.[29,33,34]

3 Results

In Table 3, we summarize the outcomes of 4000 trajectories, for two isotopic variants of the reaction. H-on-D refers to an H atom incident on a D-covered surface, and analogously for D-on-H. Primary reactions are those between the incident atom and the adsorbates producing HD, whereas secondary reactions occur between adsorbates producing H_2 or D_2. The incoming atom is at normal incidence, and the coverage is 0.5 atoms per unit cell in all results presented here. We see that there are not large isotope effects with regard to primary reactions and trapping, in agreement with the experiments of Rettner and Auerbach.[8] For H-on-D and D-on-H *ca.* 30–40% of the incident atoms react to form HD, in good agreement with the experimental value of $47 \pm 12\%$, which corresponds to a cross-section of *ca.* 5 Å^2.[8] Our earlier work suggested a cross-section for direct ER reaction of only *ca.* 0.5 Å^2, which suggested that much of the measured reactivity was of the hot-atom variety. Closer inspection of the reactive trajectories leading to HD shows that only about one third react with either of the two atoms adsorbed in the target unit cells. Assuming that about half of these trajectories correspond to direct ER reactions gives a direct cross-section roughly consistent with this earlier work. In the remaining reactive trajectories, the incident atom scatters from the corrugation and/or the adsorbates, is trapped into a hot-atom state, and eventually reacts with one of the other adsorbates. Below, we show that all the HD products are hot, with much energy in HD rotation, vibration and translation.

We see that about 6 and 23% of the trajectories reflect for H-on-D and D-on-H, respectively, again in reasonable agreement with our earlier single-adsorbate study[29]

Table 3 Calculated probabilities for various outcomes of scattering H or D from a D- or H-covered Cu(111) surface

outcome	D-on-H	H-on-D
reflection	0.23	0.06
trapping	0.42	0.51
primary reaction	0.28	0.41
secondary reaction	0.08	0.02

Reflection refers to the process where the incident atom is scattered back to the gas-phase, whereas trapping refers to the process where the incident atom is trapped on the surface without reacting with adsorbed atoms. Primary reaction refers to the reaction of the incident atom with an adsorbate atom, whereas in the process referred to as secondary reaction the incident atom induces a reaction between two adsorbed atoms.

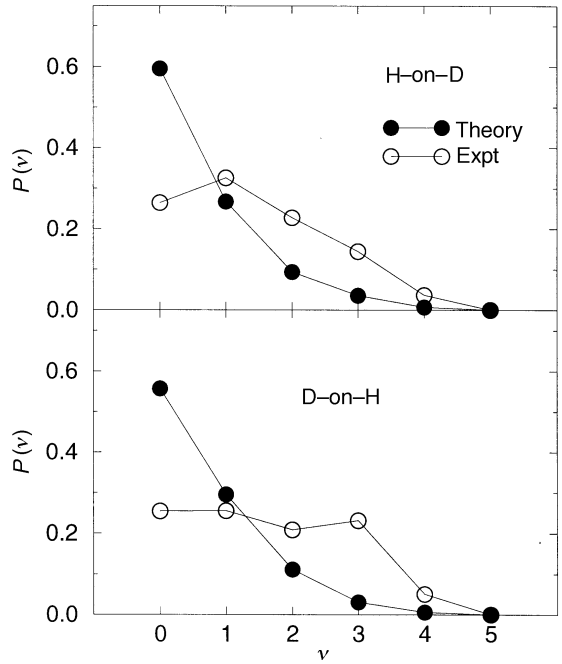

Fig. 2 Comparison between calculated and measured vibrational distributions for the HD product. H-on-D refers to the scattering of an H atom from a D-covered surface and analogously for D-on-H. The coverage is 0.5 atoms in each surface unit cell. (●) Calculated results; (○) measured and flux-corrected data taken from ref. 8.

and the experimental value, < *ca.* 10%.[8] The reflection probability for D-on-H is higher because the incident D is less perturbed by scattering from H than H is perturbed by scattering from D. Phonon interactions would lower this reflection probability a bit, particularly for D. About 40–50% of the incident atoms are trapped on the surface, but dissipate their excess energy into the adsorbates and relax without reacting by the end of the simulation, which lasts for 2.0 ps. As discussed in previous works,[26,29,33,34] the large H-metal attraction accelerates the incident atom, leading to a strong interaction with the corrugation. The relatively small asymptotic normal translational energy is easily transferred to lateral translational motion, trapping the atom. Because the adsorbates are weakly bound parallel to the surface and have masses equal or close to that of the incident atom, energy transfer from the accelerated incident atom to the adsorbates is highly efficient, leading to both trapping and energy loss. As a result, a majority of the incident atoms are trapped on the surface, with about half of them eventually reacting to form hot products, and the other half relaxing without reaction, consistent with the scenario proposed by Rettner and Auerbach.[8]

Because of this efficient energy transfer from the incident to the adsorbed atoms, we observe that adsorbates can be knocked out of the threefold sites they occupy, going on to react with other adsorbates. Since we do not observe, for a given trajectory, *e.g.* for H-on-D, the formation of both HD and D_2, we conclude that when an incident H hits D and knocks it loose, the H loses so much of its energy that it quickly relaxes without reacting. Thus, the total percentage of trajectories in which the incident atom becomes trapped without itself reacting includes these reactive trajectories and is *ca.* 50%. Rettner and Auerbach did not look for H_2 and D_2 in their H-on-D and D-on-H experiments, but these secondary processes have been seen on other metal surfaces. Winkler and co-workers,[14] for example, see *ca.* 4% D_2 for H-on-D/Ni(110), and *ca.* 6% $H_2$for D-on-

H/Ni(110), consistent with our observations. On Al(100), they observed these secondary reactions in *ca.* 10% of the scattering events. Küppers and co-workers see similar behaviour on Ni(100) and Pt(111).[17] Similar to Winkler and co-worker's study on Ni(110), we see 2% and 8% for H-on-D and D-on-H, respectively. An incident D is much more likely to knock an adsorbed H out of its site than for the opposite isotopic combination, leading to more secondary reactions for this configuration.

Rettner and Auerbach measured detailed ro-vibrational HD product distributions, and we compare our results with these distributions in Fig. 2 and 3. As in the experiments, we see a lot of vibrational excitation in the products. However, as in our earlier single-adsorbate quasi-classical studies, we see less vibrational excitation than in the experiments. For H-on-D and D-on-H we find an average HD vibrational energy of 0.49 and 0.51 eV, respectively, whereas the experimental values are 0.83 and 0.91 eV, including zero-point energy. This result is the only notable deviation from the work of Rettner and Auerbach, although it is not severe. The reasons for this deviation are not clear. In our earlier flat-surface single-adsorbate studies,[24–26] we observed a tendency for the quasi-classical results to give less vibrational excitation than the quantum calculations. Of course, the origin may also be errors in the model PES. Finally, we note that our preliminary analysis of the HD product ignores stretching of the bond length by anharmonicity and centrifugal distortion, which would tend to make the vibrational distribution broader.

The overall rotational distribution, summed over all vibrational states, is in excellent agreement with the experiments. We note that our previous single-adsorbate results[26] lead to more rotational excitation than we find here. This is because the hot-atom products have less rotational energy than those from direct ER. If one looks more closely at the rotational distributions for each individual vibrational state, one observes agreement with experiment for the general shape, but the magnitudes differ owing to the increased

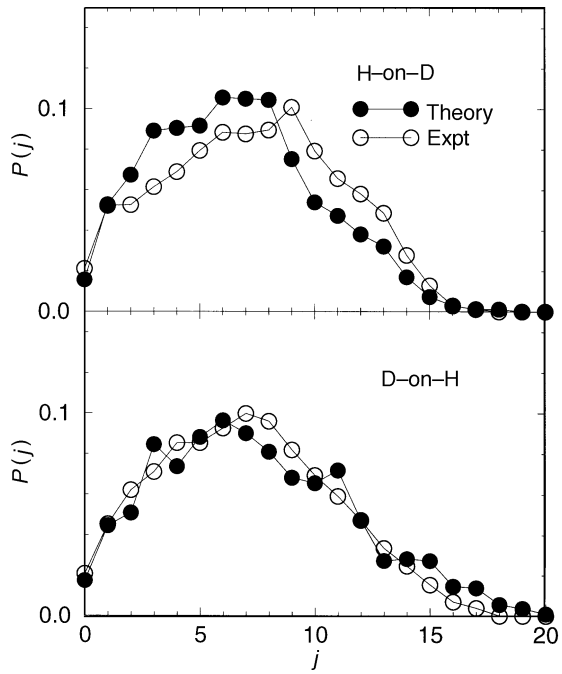

Fig. 3 Comparison between calculated and measured rotational distributions for the HD product. Symbols as in Fig. 2

vibrational excitation seen in the experiments. As in the experiments, we see only small isotope effects in the rotational and vibrational distributions, and we see some anti-correlation between rotational and vibrational excitation.

In Fig. 4, we plot the internal (ro-vibrational) energy distribution for the product HD molecules. For H-on-D and D-on-H we find that the average internal energy is 0.84 and 0.96 eV, respectively, compared with 1.2 and 1.3 eV, respectively, from the experiments (including vibrational zero-point energy). The distribution is a bit broader and extends to lower energies than in our earlier single-adsorbate studies,[26] since the hot-atoms can dissipate energy, and occasionally gain some energy from the adsorbates. As in the experiments, we see roughly half the available energy in internal product motion, and about half in centre-of-mass translation. We calculate average HD translational energies of 1.1 and 1.2 eV for H-on-D and D-on-H, respectively.

In Fig. 5, we plot the total product HD energy distribution, which would be a delta function at 2.34 and 2.39 eV for H-on-D and D-on-H, respectively, if there were no energy exchange with the other adsorbates during the reaction. These energies include the potential-energy release in the reaction (2.16 eV in our model PES), the incident energy, and adsorbate zero-point energy. We find that our distributions peak near these values, falling off rapidly above them and with longer tails to lower values. We thus see much more energy loss than gain by the hot-atom, as it scatters from one or more adsorbates prior to reaction, and for H-on-D and D-on-H the average total energy is 2.0 and 2.2 eV, respectively. The energy gain is physically incorrect and results from our quasi-classical approach, which allows the large zero-point vibrational energies of the adsorbates to be (improperly) transferred to the incident atom. Our quasi-classical methods probably overestimate energy exchange with the adsorbates in general, since the vibrational spacings, at least for vibration normal to the surface, are relatively large compared to the energy transfer. Given this effect, one might expect that the product

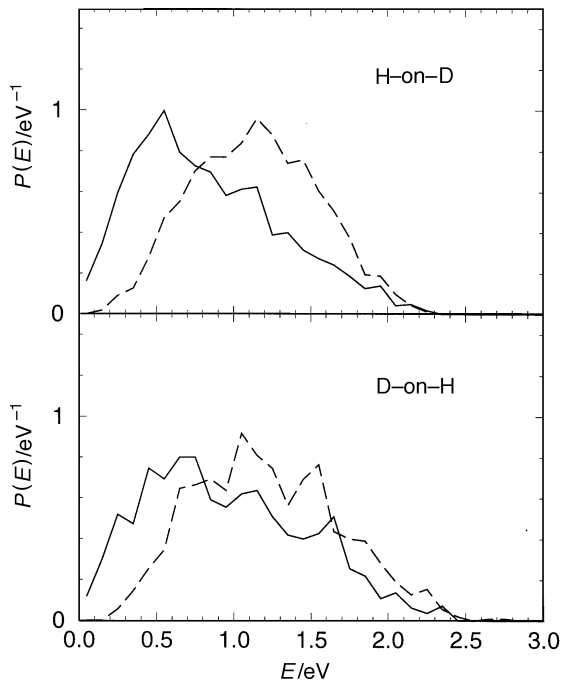

Fig. 4 Calculated internal (ro-vibrational) and translational energy distribution for the HD product. (——) internal and (— — –) translational energy distribution.

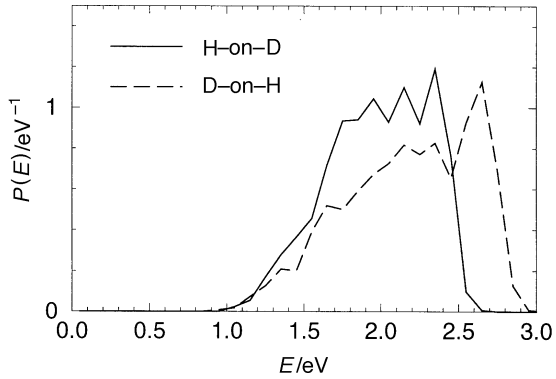

Fig. 5 Calculated total energy distribution of the HD product

translational energies would be somewhat smaller than those computed here, an argument consistent with the values measured in an earlier experiment by Rettner.[5] We note that no one has measured the total product energy for this reaction, although there is some loss to the adsorbates and/or the lattice for the H + Cl/Au(111) reaction.[6,7]

4 Concluding remarks

We have performed a quasi-classical molecular dynamics study of the reaction dynamics of HD formation by H or D atoms incident from the gas phase on a D or H-covered Cu(111) surface. A key ingredient has been the construction of a model PES for the interaction of H atoms over this surface that has been based exclusively on results from first-principle total energy calculations. These calculations were performed within DFT using the plane-wave and pseudo-potential method and the GGA for the exchange correlation energy. The calculated energy points for various relevant configurations of the H atoms over Cu(111) was used to determine all the potential parameters of a corrugated LEPS-PES, which contains one and two-body terms. We found that, at the coverage of interest, 0.5 atoms for each surface unit cell, it is sufficient to keep only one and two-body terms. Using quasi-classical molecular dynamics and this many-body PES, we have calculated probabilities for various outcomes such as reflection, trapping without reaction and reactions. We have also determined the state of the HD product, such as its translational and internal energy and vibrational and rotational excitation. The term quasi-classical refers to the fact that it is necessary to account for the zero-point vibrational motion of the adsorbates and that we have assigned vibrational and rotational quantum numbers to the ro-vibrational state of the HD product through a quantum-classical correspondence. No phonon or non-adiabatic electronic effects are included in this study.

Our preliminary study supports the scenario for the reaction dynamics proposed by Rettner and Auerbach in their unique state-resolved molecular beam studies of this reaction. In this scenario, a significant fraction of the reactions occur *via* hot-atom pathways, as opposed to ER pathways in which the incident atom reacts directly with the adsorbed atom. We draw this conclusion from the good agreement between the calculated reaction probabilities for the two isotopic cases with their measured values, and that the corresponding cross-sections are almost an order of magnitude larger than the calculated values for the ER pathway. We find that reaction pathways are much more ER-like than Langmuir–Hinshelwood-like, in the sense that there is a lot of ro-vibrational and translational energy in the HD product, which is characteristic of the large exothermicity of *ca.* 2.5 eV for ER pathways. The calculated rotational distribu-

tions for the two isotopic cases are in very good agreement with the measured ones, while the agreement with experiment is not as stunning for the vibrational distributions. In addition to these primary reactions, we find that the incident atom induces secondary reactions among the adsorbates, producing either H_2 or D_2 molecules. These kind of reactions have been seen on other metal surfaces by Winkler and co-workers and also by Küppers and co-workers. The magnitude and the isotope dependence of the calculated secondary reaction probabilities are in good agreement with their measured values.

In the future, we plan to examine in more detail the nature of the reaction pathways and to calculate product distributions that can be compared with all available experimental data such as, for instance, angular distributions. In particular, we would like to understand if the discrepancy between the calculated and measured vibrational distributions is caused by the quasi-classical approximation or by details of the PES. There is still room for improvement of the PES. For instance, the fit of the corrugated LEPS-PES to the calculated total energies is not perfect: a root-mean-square error of *ca.* 0.2 eV, which should be able to be improved by developing a more sophisticated model PES. Finally, it would be interesting to include phonon (and non-adiabatic electronic) effects in the calculation that should influence the hot-atom pathways at lower coverages.

M.P. is grateful for support by the Swedish Natural Science Research Council (NFR). D.S. and B.J. gratefully acknowledge support from the Division of Chemical Sciences, Office of Basic Energy Sciences, Office of Energy Research, U.S. Department of Energy, under Grant No. DE-FG02-87ER13744. We are also grateful to B. Hammer and D. M. Bird for sharing their experiences of density functional calculations with us. Allocation of computer resources at the center of parallel computing (PDC) is gratefully acknowledged.

References

1 R. I. Hall, I. Cadez, M. Landau, F. Pichou and C. Schermann, *Phys. Rev. Lett.*, 1998, **60**, 337.
2 C. J. Eenshustra, J. H. M. Bonnie, J. Los and H. J. Hopmann, *Phys. Rev. Lett.*, 1988, **60**, 341.
3 K. R. Lykke and B. D. Kay, in *Laser Photoionization and Desorption Surface Analysis Techniques*, ed. N. S. Nogar, Society of Photo Optical Instrumentation Engineers 1208, 1990, p. 18.
4 E. W. Kuipers, A. Vardi, A. Danon and A. Amirav, *Phys. Rev. Lett.*, 1991, **66**, 116.
5 C. T. Rettner, *Phys. Rev. Lett.*, 1992, **69**, 383.
6 C. T. Rettner and D. J. Auerbach, *Science*, 1994, **263**, 365.
7 C. T. Rettner, *J. Chem. Phys.*, 1994, **101**, 1529.
8 C. T. Rettner and D. J. Auerbach, *Phys. Rev. Lett.*, 1995, **74**, 4551; *J. Chem. Phys.*, 1996, **104**, 2732; *Surf. Sci.*, 1996, **357–358**, 602.
9 D. D. Koleske, S. M. Gates and J. A. Schultz, *J. Chem. Phys.*, 1993, **99**, 5619.
10 D. D. Koleske, S. M. Gates and B. Jackson, *J. Chem. Phys.*, 1994, **101**, 3301.
11 C. C. Cheng, S. R. Lucas, H. Gutleben, W. J. Choyke and J. T. Yates Jr., *J. Am. Chem. Soc.*, 1992, **114**, 1429.
12 S. A. Buntin, *J. Chem. Phys.*, 1996, **105**, 2066.
13 T. A. Jachimowski and W. H. Weinberg, *J. Chem. Phys.*, 1994, **101**, 10997.
14 G. Eilmsteiner, W. Walkner and A. Winkler, *Surf. Sci.*, 1996, **352–354**, 263; G. Eilmsteiner and A. Winkler, *Surf. Sci.*, 1996, **366**, L750; J. Boh, G. Eilmsteiner, K. D. Rendulic and A. Winkler, *Surf. Sci.*, 1998, **395**, 98.
15 M. Xi and B. E. Bent, *J. Chem. Phys.*, 1993, **97**, 4167.
16 J. B. U. A. Schubert, A. Schenk, B. Winter, C. Lutterloh and J. Küppers, *J. Chem. Phys.*, 1993, **99**, 3125; C. Lutterloh, A. Schenk, J. Biener, B. Winter and J. Küppers, *Surf. Sci.*, 1994, **316**, L1039; C. Lutterloh, J. Biener, A. Schenk and J. Küppers, *Surf. Sci.*, 1995, **331–333**, 261; *J. Chem. Phys.*, 1996; **104**, 2392; J. Biener, C. Lutterloh, A. Schenk, K. Pöhlmann and J. Küppers, *Surf. Sci.*, 1996, **365**, 255.
17 S. Wehner and J. Küppers, *J. Chem. Phys.*, 1998, **108**, 3353; Th. Kammler, J. Lee and J. Küppers, *J. Chem. Phys.*, 1997, **106**, 7362.
18 Y.-S. Park, J.-Y Kim and J. Lee, *Surf. Sci.*, 1996, **363**, 62.
19 B. D. Thomas, J. J. N. Russel, P. E. Pehrsson and J. Butler, *J. Chem. Phys.*, 1994, **100**, 8425.
20 C. T. Rettner, D. J. Auerbach and J. Lee, *J. Chem. Phys.*, 1996, **105**, 10115.

21 P. Kratzer and W. Brenig, *Surf. Sci.*, 1991, **254**, 275.
22 B. Jackson and M. Persson, *J. Chem. Phys.*, 1992, **96**, 2378; *Surf. Sci.*, 1992, **269–270**, 195.
23 B. Jackson, M. Persson and B. D. Kay, *J. Chem. Phys.*, 1994, **100**, 7687.
24 M. Persson and B. Jackson, *J. Chem. Phys.*, 1995, **102**, 1078.
25 M. Persson and B. Jackson, *Chem. Phys. Lett.*, 1995, **237**, 468.
26 B. Jackson and M. Persson, *J. Chem. Phys.*, 1995, **103**, 6257.
27 B. Jackson and M. Persson, in *Elementary Processes in Excitations and Reactions on Solid Surfaces*, ed. A. Okiji, H. Kasai and K. Makoshi, Springer Series in Solid-State Sciences, Vol. 121, Springer-Verlag, Berlin, 1996.
28 P. Kratzer and W. Brenig, *Z. Phys. B*, 1996, **99**, 571.
29 S. Caratzoulas, B. Jackson and M. Persson, *J. Chem. Phys.*, 1997, **107**, 6420.
30 P. Kratzer, *J. Chem. Phys.*, 1997, **106**, 6752.
31 G. R. Darling and S. Holloway, *Rep. Prog. Phys.*, 1995, **58**, 1595.
32 J. Harris and B. Kasemo, *Surf. Sci.*, 1981, **105**, L281.
33 J. Strömqvist, L. Bengtsson, M. Persson and B. Hammer, *Surf. Sci.*, 1998, **397**, 382.
34 D. Shalashilin and B. Jackson, *J. Chem. Phys.*, in press.
35 B. Hammer, M. Scheffler, K. Jacobsen and J. K. Nørskov, *Phys. Rev. Lett.*, 1994, **73**, 1400.
36 J. A. White, D. M. Bird, M. C. Payne and I. Stich, *Phys. Rev. Lett.*, 1994, **73**, 1404; J. A. White, D. M. Bird and M. C. Payne, *Phys. Rev. B*, 1996, **53**, 1667; S. Wilke and M. Scheffler, *Surf. Sci.*, 1995, **329**, L605; G. Wiesenekker, G. J. Kroes, E. J. Baerends and R. C. Mowrey, *J. Chem. Phys.*, 1995, **102**, 3873; 1995, **103**, 5168 (E).
37 J. H. McCreery and J. Wolken Jr., *J. Chem. Phys.*, 1977, **67**, 2551.
38 DACAPO version 1.18, B. Hammer, CAMP, Technical University, Denmark.
39 M. Persson, J. Strömqvist, L. Bengtsson, B. Jackson, D. Shalashilin and B. Hammer, *J. Chem. Phys.*, submitted.
40 The first four sets of fourier terms, each set having the same coefficient, are $(h,k) = (0,0)$; $(-1,1)$, $(-1,0)$, $(0,1)$, $(0,-1)$, $(1,0)$, $(1,-1)$; $(-2,1)$, $(-1,2)$, $(-1,-1)$, $(1,1)$, $(1,-2)$, $(2,-1)$ and $(-2,2)$, $(-2,0)$, $(0,2)$, $(0,-2)$, $(2,0)$, $(2,-2)$.
41 B. I. Dunlap, in *Ab initio Methods in Quantum Chemistry-II*, ed. K. P. Lawley, Wiley, 1987, p. 287.
42 We have tested the convergence with respect both to the number of k-points and the cut-off in kinetic energy for the plane waves in the super cell. For the standard cut-off of 50 Ry, an increase in the number of k points by a factor of three increases the total energy of the isolated molecule at $r = 0.75$ Å by less than 0.012 eV. For the values of 50, 60, 70 and 80 Ry for the cut-off the calculated energies of the spin-polarized H atom are -13.542, -13.555, -13.572 and -13.584, respectively, and the corresponding binding energies of the isolated molecule at $r = 0.75$ Å are 4.471, 4.499, 4.508 and 4.516 eV, respectively.
43 J. Dai and J. Z. H. Zhang, *J. Chem. Phys.*, 1995, **102**, 6280.

Paper 8/01130C; *Received* 9*th February*, 1998